RiESTech
Recent in Engineering Science and Technology

MBI

Article

Influence of Moringa Leaf and Purple Sweet Potato Extract Concentrations on the Inhibition Efficiency of API 5L Steel in Acidic Medium

Kezia [1], Yudha Pratesa [1,*], Tio Angger Pertama [1], Johny Wahyuadi Soedarsono [1]

[1] Department of Metallurgical and Materials Engineering, Universitas Indonesia, Depok, Indonesia 16424
* Correspondence: yudhapratesa@ui.ac.id

Abstract: This study aimed to investigate the corrosion inhibition mechanism of moringa leaves extract (Moringa oleifera) and purple sweet potato extract (Ipomoea batatas) extract as environmentally friendly inhibitors for low carbon API 5L steel in a 0.2 M HCl solution. Potentiodynamic polarization and electrochemical impedance spectroscopy (EIS) tests were conducted with varying concentrations and combinations of the two inhibitors to evaluate their corrosion inhibition performance. The results indicated that both inhibitors individually function effectively as green corrosion inhibitors. However, their combination did not offer adequate protection for API 5L steel in a 0.2 M HCl environment. FTIR analysis of the inhibitors confirmed the presence of flavonoid compounds in both extracts. Potentiodynamic polarization tests showed that increasing the concentration of moringa leaves extract resulted in a decrease in the corrosion rate and an increase in %IE, with the highest efficiency reaching 73.08%. Similarly, an increase in the volume of purple sweet potato extract also resulted in a reduced corrosion rate, with a maximum inhibition efficiency of 65.31%. However, the combination of both inhibitors led to an increase in the corrosion rate. The results of the EIS test demonstrated that both inhibitors protect the metal by forming a protective film layer on its surface. The adsorption behavior of the inhibitors corresponds to a physical adsorption process and aligns with the Langmuir adsorption isotherm model.

Keywords: Moringa leaves; Purple sweet potato; FTIR; Potentiodynamic polarization; EIS

Citation: Kezia, Pratesa, Y., Pertama, T. A., Soedarsono, J. W. (2025). Influence of Moringa Leaf and Purple Sweet Potato Extract Concentrations on the Inhibition Efficiency of API 5L Steel in Acidic Medium. Recent in Engineering Science and Technology, 3(04), 36–48. Retrieved from https://www.mbi-journals.com/index.php/riestech/article/view/120

Academic Editor: Vika Rizka

Received: 22 June 2025
Accepted: 6 September 2025
Published: 31 October 2025

1. Introduction

Corrosion is the detrimental outcome of a chemical reaction between a metal or alloy and its surrounding environment [1]. It poses a significant challenge and is commonly encountered across various industrial sectors. The corrosion problems will decrease the quality of equipment or facilities that may affect the final product and work safety. One method that can be done to control corrosion in ferrous materials such as steel is to use corrosion inhibitors. Corrosion inhibitors are compounds added to environments with small concentrations that can decrease corrosion rates in metals [2]. Nowadays the concern for the environment is increasing, this affects the selection of inhibitors. Green corrosion inhibitors are optional because they are non-toxic, biodegradable, safe for human and environment.

Green corrosion inhibitors are made from plant and grain extracts. Plant extracts such as skin, leaves and stems may inhibit the corrosion rate because it contains heterocyclic compounds such as alkaloids, flavonoids, nicotine, hydrazine, alanine, quinolone, aniline, pyridine and others. In this study, extracts from moringa leaves (Moringa oleifera) and purple sweet potato (Ipomoea batatas) were used as green corrosion inhibitors.

Moringa oleifera or Kelor in Bahasa Indonesia is belong to Moringaceae family that is distributed mostly in tropical and subtropical regions. Moringa products, from leaves, flowers to seeds, contain a number of macronutrients that are known to be good for the health of the body. In addition, moringa leaves contain antioxidants such as tannins, triterpenoid steroids, flavonoids, saponins, anthraquinones, and alkaloids [3]. This conditions makes kelor potential to be used as green corrosion inhibitor. Research done by Subasree et al. found that moringa leaves can be used as green corrosion inhibitor for low carbon steel in 1M H2SO4 [4]. The inhibition efficiency (IE) increased with increasing extract concentration, IE 96% was observed with 8 ml of plant extract in acidic media.

Purple sweet potato (Ipomoea batatas) is well known for its antioxidant content. It is called 'purple' due to the characteristic color of the tuber and belongs to the Convolvulaceae family. The antioxidant properties of purple sweet potato are largely attributed to anthocyanins. Anthocyanins are key compounds in purple sweet potatoes, derived from a monoaromatic structure known as cyanidin. Anthocyanins are derived from cyanidin, either through the addition or removal of hydroxyl groups or by methylation. Anthocyanins are also recognized for their antioxidant properties. A study conducted by Ayende et al. found that purple sweet potato extract can reduce the corrosion rate of API 5L steel in produced water [5].

This research is done to see the inhibition mechanism of moringa, purple sweet potato and combination between moringa and purple sweet potato.

2. Materials and Experiment Methods

2.1. Preparation of the test solution

The test solution used in this study was 0.2 M HCl. It prepared from 864 ml of 37% HCl and dissolved in 136 ml distilled water. Two types of inhibitors were used: moringa leaf extract and purple sweet potato extract, each at concentrations of 0, 1000, 2000, 3000, 4000, and 5000 ppm. In addition, purple sweet potato extract at various concentrations was combined with moringa leaf extract at a fixed concentration of 5000 ppm.

2.2. Specimen preparation

This study used API 5L with chemical composition was as follows (wt%): 0.193% C, 0.309% Si, 0.404% Mn, 0.013% P, 0.012% S, 0.024 Cr, 0.027% Mo, 0.035% Ni, 0.008% Al, 0.119% Cu, 0.004% Nb, 0.004% Ti, 0.007% V and Fe balance. It was tested with using Optical Emission Spectroscopy (OES). The specimen was 10 mm in diameter exposed surface area and mounted using epoxy resin. The exposed area was wet polished with 200, 400 and 600 SiC paper until previous coarse scratch by sectioning are removed, then it was rinsed with distilled water and dried. This process was repeated in every potentiodynamic testing.

2.3. Electrochemical measurement

A conventional three-electrode cell was used for all electrochemical measurements. The API 5L specimen served as the working electrode, with a platinum sheet as the counter electrode. The cell potential was measured against a saturated calomel electrode (SCE) as the reference. The working electrode was prepared in the form of a cylindrical API 5L rod, embedded in araldite, with an exposed bottom surface area of 0.785 cm^2 in contact with 500 mL of 0.2 M HCl electrolyte.

Potentiodynamic experiments were conducted at a scan rate of 1 mV/s, with a scan range from -1 V to +2 V relative to the open circuit potential (OCP). Tafel curves were extrapolated to the corrosion potential to calculate the electrochemical kinetic parameters. The IE were obtained by using Equation (1):

$$IE = \left[1 - \left(\frac{i_{corr\,(i)}}{i_{corr\,(o)}}\right)\right] x\ 100\% \qquad (1)$$

where icorr (o) and i corr (i) represent the corrosion current densities of the specimen in the absence and presence of various concentrations of the inhibitor, respectively.

EIS measurements were conducted to determine the polarization resistance (Rct) and double layer capacitance (Cdl). The study was carried out using a potential amplitude of 10 mV, with a frequency range from 10 kHz to 0.1 Hz. The inhibition efficiency (IE) was calculated using Equation (2):

$$IE = \left[1 - \left(\frac{R_{ct\,(i)}}{R_{ct\,(o)}}\right)\right] x\ 100\% \qquad (2)$$

where Rct (o) and Rct (i) represent the charge transfer resistance of the specimen in the absence and presence of the inhibitors, respectively.

2.4. Fourier Transform Infrared (FTIR) testing

FTIR testing was conducted to identify the types of functional groups present in the organic compounds, such as alcohols, alkaloids, and free elements containing nitrogen (N), oxygen (O), phosphorus (P), and sulfur (S).

3. Results and Discussion

3.1. Potentiodynamic Polarization

Tafel plots of the API 5L electrode in 0.2 M HCl solution with varying concentrations of moringa leaf extract, purple sweet potato extract, and their combination are presented in Figure 1.

The electrochemical parameters, i.e., corrosion potential (Ecorr), corrosion current density (icorr), anodic (βa) and cathodic (βc) slopes shown in Table 1-3, were collected from tafel plots and polarization resistance experiments carried out separately. Table 1 shows that the value of Ecorr has changed in both positive and negative directions, which means that anodic dissolution of metals and cathodic reduction of hydrogen ions have decreased due to the adsorption of moringa extract on the anodic and cathodic parts of the metal surface.

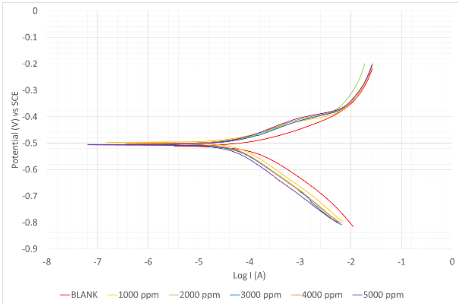

(a)

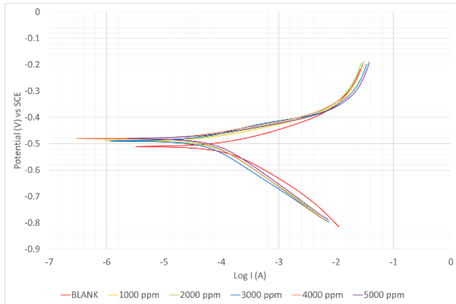

(b)

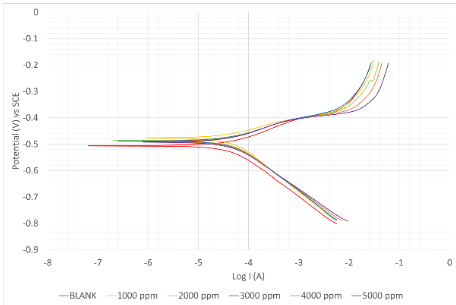

(c)

Figure. 1. Polarization curves of API 5L in different inhibitor concentration **(a)** Moringa leaves extract; **(b)** Purple sweet potato extract; **(c)** Combination of both.

In other words, these inhibitors belong to the mixed-type inhibitor category [6]. Changes in the value of Ecorr with and without the addition of inhibitors greater than 85 mV in either the anodic or cathodic direction indicate that the inhibitors belong to the anodic or cathodic inhibitor type. However, if the change in Ecorr between the absence and presence of inhibitors is less than 85 mV, the inhibitors are classified as mixed-type inhibitors [7]. This study showed a maximum change in Ecorr of 19 mV, indicating that Moringa extract belong to the mixed-type inhibitor category. This finding is further supported by research conducted by Fouda et al., who reported a maximum Ecorr shift of 48 mV when using moringa leaves extract as an inhibitor in 2 M HCl [16].

The value of icorr also with increasing inhibitor concentration due to a larger surface area of the electrode being covered by the inhibitors. This phenomenon contributes to a reduction in the corrosion rate. Additionally, decreases in the values of βc and βa are observed with increasing inhibitor concentration, indicating that both the anodic dissolution of metals and cathodic reduction of hydrogen ions have been suppressed due to the adsorption of Moringa leaves extract inhibitors on the anodic and cathodic regions of the steel surface [8].

Table 2 shows the electrochemical parameters for API 5L in the absence and presence of purple sweet potato extract. A maximum change in Ecorr by 31 mV indicates that purple sweet potato extract inhibitors belong mixed inhibitor type. A similar conclusion was also drawn from the application of purple sweet potato extract in a 3.5% NaCl environment [17].

Table 1. Electrochemical parameters for API 5L in moringa leaves extract inhibitor.

C (ppm)	E_{corr} (mV vs SCE)	i_{corr} (μA/cm²)	β_c (mV/dec)	β_a (mV/dec)	CR (mpy)	%EI
0	-511	211,00	1,73 x 10^3	1,25 x 10^{-3}	123	0,00
1000	-492	89,30	1,61 x 10^3	1,06 x 10^{-3}	52,02	57,68
2000	-505	86,10	1,68 x 10^3	1,18 x 10^{-3}	50,20	59,19
3000	-506	86,30	1,71 x 10^3	1,08 x 10^{-3}	50,31	59,10
4000	-502	78,30	1,64 x 10^3	1,06 x 10^{-3}	45,64	62,89
5000	-506	56,80	1,55 x 10^3	1,02 x 10^{-3}	33,13	73,08

Table 2. Electrochemical parameters for API 5L in purple sweet potato inhibitor.

C (ppm)	E_{corr} (mV vs SCE)	i_{corr} (μA/cm²)	β_c (mV/dec)	β_a (mV/dec)	CR (mpy)	%EI
0	-511	211,00	1,73 x 10^3	1,25 x 10^{-3}	123	0,00
1000	-490	114,00	1,80 x 10^3	1,07 x 10^{-3}	66,51	45,97
2000	-488	103,00	1,74 x 10^3	1,09 x 10^{-3}	60,25	51,18
3000	-489	73,20	1,60 x 10^3	9,91 x 10^{-3}	42,69	65,31
4000	-481	88,20	1,73 x 10^3	1,04 x 10^{-3}	51,38	58,20
5000	-480	109,00	1,77 x 10^3	1,03 x 10^{-3}	63,51	48,34

Table 3. Electrochemical parameters for API 5L in combination of both inhibitors.

C (ppm)		E_{corr} (mV vs SCE)	i_{corr} (μA/cm²)	β_c (mV/dec)	β_a (mV/dec)	CR (mpy)	%EI
Moringa leaves	Purple sweet potato						
5000	-	-506	56,80	1,55 x 10^3	1,02 x 10^{-3}	33,33	0,00
5000	1000	-477	68,10	1,75 x 10^3	9,97 x 10^{-3}	39,69	-19,89
5000	2000	-486	69,70	1,65 x 10^3	9,83 x 10^{-3}	40,61	-22,71
5000	3000	-488	70,80	1,64 x 10^3	1,03 x 10^{-3}	41,25	-24,65
5000	4000	-490	65,20	1,53 x 10^3	9,60 x 10^{-3}	38,02	-14,79
5000	5000	-492	57,10	1,42 x 10^3	9,05 x 10^{-3}	33,28	-0,53

Furthermore the value of icorr also decreases with the addition of purple sweet potato extract, with the optimum decrease observed at 3000 ppm. The decrease in corrosion rate is caused by the presence of anthocyanin compounds in purple sweet potatoes, as reported in the research of Ayende et al. [5]. In their research, Ayende et al. also found that the inhibition efficiency of purple sweet potato extract was unstable [9]. Meanwhile, anthocyanin compounds extracted from cherries have been shown to inhibit corrosion in acidic media by up to 94.44% [18].

Furthermore, purple sweet potato extract with varying concentrations was added to moringa leaves extract with a concentration of 5000 ppm. Purple sweet potato, which is rich in anthocyanins, has the ability to resist oxidation and is therefore expected to synergistically enhance inhibitor efficiency by forming a relatively dense protective film [19]. The electrochemical parameter of mixture inhibitor as shown in Table 3. The value of icorr increases with the addition of purple sweet potato extract, this results in an increased corrosion rate, causing the inhibition efficiency to decrease as the concentration of purple sweet potato extract increases. In a study conducted by Wijaya et al. [17], the addition of 2 mL of purple sweet potato extract to curcumin extract was proven to enhance inhibitor efficiency. However, the efficiency of the mixture decreased when a higher amount of purple sweet potato extract was added. A similar trend was observed with the use of purple sweet potato extract as both a standalone and mixed inhibitor in 0.2 M HCl solution, where the efficiency decreased after the concentration exceeded the optimum level [20].

3.2. Electrochemical Impedance Spectroscopy (EIS)

The Nyquist plots obtained from the EIS measurement in the absence and presence of the inhibitors are shown in Figures 2. The diameter of the semicircle on the Nyquist curve can be used as an indicator of the inhibitor's effectiveness in preventing corrosion. The larger the diameter of the semicircular arc, the greater the inhibitor's ability to protect the metal from corrosion [21, 27]. These curves do not form perfect semicircles, which can be attributed to frequency dispersion. This phenomenon is often associated with surface roughness and inhomogeneity of the electrode surface [22]. The figures show that the Nyquist plot shapes for all three inhibitors are comparable. Across all concentrations, the plots consistently display a single depressed semicircle, suggesting that the addition of inhibitors does not significantly alter the corrosion mechanism [10].

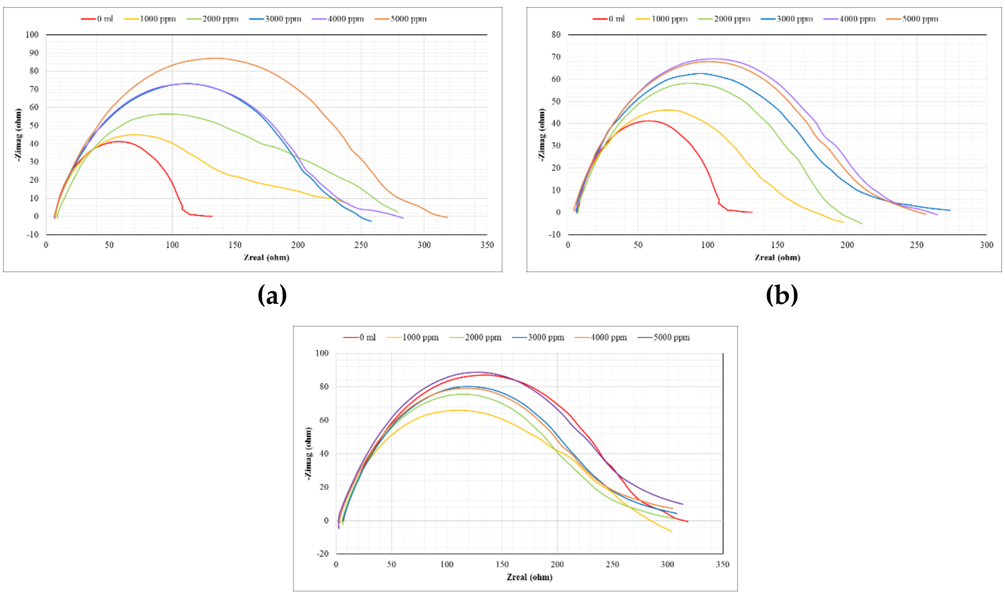

(a) **(b)**

(c)

Figure. 2. Nyquist plots in the absence and presence of inhibitor **(a)** Moringa leaves extract; **(b)** Purple sweet potato extract; **(c)** Combination of both.

Various parameters obtained from impedance measurements are given in Table 4-6. The charge transfer resistance (Rct) reflects the resistance to electron transfer at the metal surface and is inversely related to the corrosion rate [11]. To achieve a more accurate model, a constant phase element (CPE) is used in place of an ideal double-layer capacitor in the equivalent circuit (Figure 3) [12]. This element accounts for surface irregularities on the electrode, contributing to the depressed semicircle observed in Nyquist plots, as the metal–electrolyte interface behaves like a capacitor with a non-uniform surface.

Table 4 and 5 show that the value of Rct increases with the addition of moringa extract and purple sweet potato extract but not with the combination of both (Table 6). The increase in Rct values could be attributed to the formation of a protective electrochemical double layer on the metal-solution interface [13]. The proportional increase in Rct with the volume of moringa extract added indicates a rise in surface coverage, meaning a larger portion of the metal surface is being covered by the protective film. This is further supported by the increase in inhibition efficiency, which reaches up to 60.60%. For comparison, the inhibition efficiency of moringa leaves extract is slightly lower than that of neem leaf extract (69.3%), pawpaw leaf extract (68.4%), and curry leaf extract (64.6%) as reported by Chukwueze et al. [23] aslo curcuma xanthorrhiza extract that obtained 90% efficiency inhibition [28]. The inhibition efficiency, calculated from EIS results, shows the same trend as that obtained from polarization measurements.

Table 4. Impedance parameters and inhibition efficiency for API 5L in moringa leaves extract inhibitor.

C (ppm)	R_s (Ω.cm^2)	R_{ct} (Ω.cm^2)	CPE (μS.s^n)	n	C_{dl} (μF.cm^{-2})	X^2	EI (%)
0	6.644	106.5	172.1	0.846	1,027.57	0.001	0
1000	7.758	147.6	180.8	0.843	1,206.56	0.214	27.85
2000	8.601	218.3	476.5	0.702	64,244.52	0.005	51.21
3000	6.450	221.2	196.8	0.768	4,958.29	0.001	51.85
4000	6.391	226	200.1	0.775	4,495.75	0.003	52.88
5000	6.374	270.3	196.2	0.762	5,866.03	0.001	60.60

Table 5. Impedance parameters and inhibition efficiency for API 5L in purple sweet potato extract inhibitor.

C (ppm)	R_s (Ω.cm^2)	R_{ct} (Ω.cm^2)	CPE (μS.s^n)	n	C_{dl} (μF.cm^{-2})	X^2	EI (%)
0	6.644	106.5	172.1	0.846	1,027.57	0.001	0
1000	5.319	150.6	299.9	0.76	8,849.40	0.003	29.28
2000	6.736	169.3	302.7	0.843	2,281.07	0.125	37.09
3000	6.397	186.7	151.2	0.867	728.28	0.003	42.96
4000	5.062	216.8	350.8	0.763	11,513.65	0.173	50.88
5000	3.489	214.7	383.5	0.749	17,023.48	0.162	50.40

Table 6. Impedance parameters and inhibition efficiency for API 5L in combination of both inhibitors.

C (ppm)		R_s ($\Omega.cm^2$)	R_{ct} ($\Omega.cm^2$)	CPE ($\mu S.s^n$)	n	C_{dl} ($\mu F.cm^{-2}$)	X^2	EI (%)
Moringa leaves	Purple sweet potato							
5000	-	6.374	270.3	196.2	0.762	5,866.03	0.001	0
5000	1000	5.721	237.5	346.3	0.747	16,000.88	0.006	-13.81
5000	2000	5.397	240.9	299.2	0.766	9,118.78	0.028	-12.20
5000	3000	6.177	252.9	329.9	0.756	12,786.40	0.002	-6.88
5000	4000	2.871	247.4	316.4	0.77	9,161.61	0.018	-9.26
5000	5000	1.937	250.3	243.9	0.845	1,841.01	0.198	-7.99

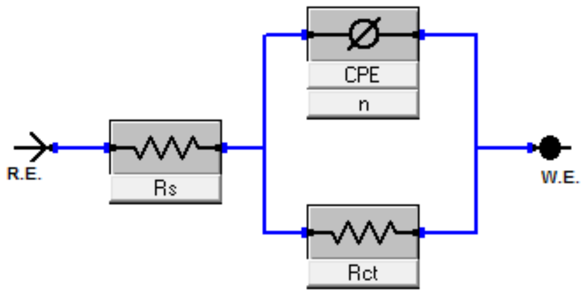

Figure. 3. The Randles circuit which is the equivalent circuit for this impedance spectra.

3.3. Fourier Transform Infrared (FTIR)

The FTIR spectrum of the moringa leaves extract, purple sweet potato extract and the combination of both are represented in Figure 4 respectively.

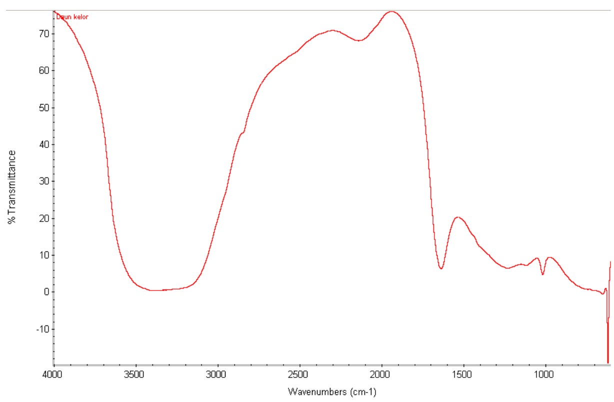

(a)

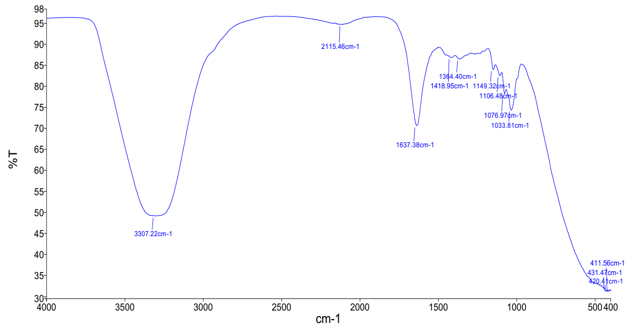

(b)

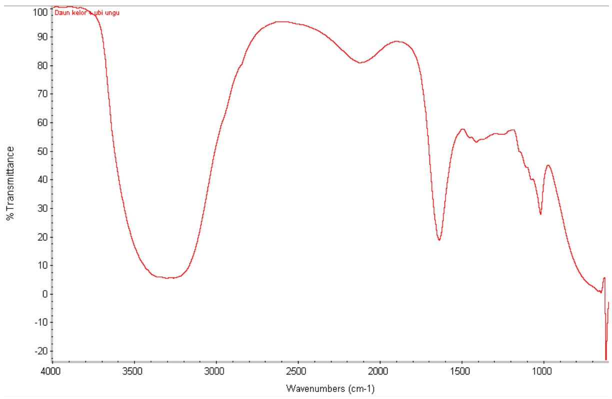

(c)

Figure. 4. Results of FTIR characterization in the absence and presence of inhibitor (a) Moringa leaves extract; (b) Purple sweet potato extract; (c) Combination of both.

FTIR is capable of revealing the distinctive characteristics of chemical bonds and molecular structures. The peaks and spectra generated by FTIR serve as unique fingerprints for identifying specific molecular structures and types of chemical bonding [24]. Figure 4(a) shows the results of FTIR characterization of moringa leaves extract solutions. A peak appears at wave number 3467 cm^{-1}, indicating O-H (COOH) acid bonds which are characteristic of alcohol and phenol compounds. Another peak at 2132 cm^{-1} indicates the presence of a C≡C bond, which is associated with alkyne compounds. Additionally, there is a spectrum peak around at 1637 cm^{-1} which indicates the C=C bond suggesting the presence of alkene compounds. Figure 4(b) shows the results of FTIR characterization of purple sweet potato extract. A peak appears at 3307.22 cm^{-1} indicating stretching O–H vibrations typical of alcohol and phenol compounds. According to Ayende et al., purple sweet potato extract contains anthocyanin components, which include OH groups [9]. Another peak at 1637.36 cm^{-1} indicates C=C vibration, , characteristic of alkene compounds. Based on these results, it can be inferred that purple sweet potato extract contains flavonoids. Figure 4(c) shows the results of FTIR characterization results for a combination of moringa extract and purple sweet potato ekstract. A peak appears at 3330 cm^{-1} indicating the presence of O-H groups from alcohol and phenol compounds. Another peak at

2120 cm^{-1} shows the presence of a C≡C bond, again associated with alkyne compounds. Additionally, a spectrum peak around 1720 cm^{-1} indicates the presence of C=C bond, suggesting alkene compounds. The FTIR analysis results reveal the presence of functional groups containing oxygen atoms and aromatic ring structures, features commonly recognized as indicators of effective corrosion inhibitors [25].

3.4. Adsorption Isotherm

The corrosion inhibition efficiency of the inhibitors on API 5L in 0.2 M HCl depends on their ability to adsorb onto the metal surface. This adsorption behavior can be quantitatively assessed through adsorption isotherm models. The coverage of moringa leaves extract and purple sweet potato extract on API 5L is defined by the following equation:

$$\theta = \frac{\eta}{100} \quad (3)$$

where η represents the inhibition efficiency of moringa leaves extract and purple sweet potato extract, as obtained from potentiodynamic polarization measurements. Several adsorption isotherm models, including Langmuir, Freundlich, Frumkin, and Temkin, have been applied to evaluate the relationship between inhibitor concentration (C) and surface coverage (θ). Among these, the adsorption behavior of the inhibitor molecules was found to best follow the Langmuir isotherm model:

$$\frac{C}{\theta} = \frac{1}{K_{ads}} + C \quad (4)$$

where Kads stands for the equilibrium constant of the adsorption process, C is the inhibitor concentration and θ represents the fraction of surface coverage. The fitting curve presented in Figure 5 exhibits a slope and correlation coefficient (R^2) that are nearly equal to 1. This slight deviation from the ideal Langmuir isotherm indicates that the adsorption layer formed by the inhibitor molecules on the metal surface is not an ideal monolayer [14].

Figure. 5. Langmuir adsorption plots of moringa leaves extract and purple sweet potato extract.

The standard free energy of adsorption $\Delta G^o ads$ is calculated using the following equation:

$$\Delta G^o ads = -RT \ln (55.5\ Kads) \quad (5)$$

where R = 8.314 J/mol.K is the universal gas constant, T is the absolute temperature, and 55.5 represents the molar concentration of water. The calculated values of $\Delta G^o ads$ were -7.419 kJ/mol for moringa extract and -4.047 kJ/mol for purple sweet potato extract. The significantly negative values indicate strong adsorption of these compounds on the steel surface. Generally, $\Delta G^o ads$ values around -20 kJ/mol or less suggest electrostatic interactions between the charged metal surface and charged organic molecules in solution, while values near -40 kJ/mol or more imply charge sharing or transfer between the metal and the organic molecules [15]. For both inhibitors the values obtained are less negative than -20 kJ/mol, indicating that the adsorption onto the steel surface is primarily physical in nature [26].

3.5. Inhibition Mechanism

From several measurements that have been done, it is shown that the inhibition mechanism of moringa leaves extract inhibitor and purple sweet potato extract on API 5L steel in 0.2 M HCl is effective. FTIR results showed that the inhibitor has an -OH functional group which has properties as an antioxidant that can bind oxygen to the environment. Then, the inhibitor is adsorbed on the metal surface physically, this is shown by the value of $\Delta G^o ads$ being more than -20 kJ/mol and from EIS testing where the Rct value increases along with the addition of the inhibitor. The compounds of the inhibitor on the metal surface form a film layer covering the surface. Furthermore, Cl^- ions from HCl solution can not react with metals because of the blocking film layer, this is shown by the potentiodynamic polarization test where the corrosion rate decreases with increasing inhibitor concentration.

4. Conclusions

Moringa leaves extract and purple sweet potato extract can be used for green corrosion inhibitor, it shown from decreasing of corrosion rate and increasing of inhibition efficiency along with the addition of the inhibitor. The highest value of inhibition efficiency for moringa leaves extract and purple sweet potato extract is 73.08% and 65.31% respectively. The combination of both extract cannot be used for green corrosion inhibitor, it shown from the value of corrosion rate increase with the addition of the inhibitor. Moringa leaves extract and purple sweet potato were physically adsorbed on the steel surface.

Author Contributions: Conceptualization, Kezia; methodology, Tio Angger Pertama; software, Tio Angger Pertama; validation, Kezia, Tio Angger Pertama, Johny Wahyuadi Soedarsono and Yudha Pratesa; formal analysis, Kezia and Tio Angger Pertama; investigation, Tio Angger Pertama; resources, Kezia and Tio Angger Pertama; data curation, Tio Angger Pertama; writing—original draft preparation, Tio Angger Pertama; writing—review and editing, Kezia; visualization, Tio Angger Pertama; supervision, Johny Wahyuadi Soedarsono; project administration, Tio Angger Pertama. All authors have read and agreed to the published version of the manuscript.

Funding: This research received no external funding.

Conflicts of Interest: The authors declare no conflict of interest. The funders had no role in the design of the study; data collection, analysis, or interpretation; manuscript writing; or decision to publish the results.

References

1. D. A. Jones, Principles and Prevention of Corrosion, New York: Macmillan Publishing Company, 1992.
2. P. R. Roberge, Corrosion Engineering: Principles and Practice, McGraw Hill, 2008.
3. J. N. Kasolo, G. S. Bimenya, L. Ojok, J. Ochieng and J. W. Ogwal-Okeng, "Phytochemicals and uses of Moringa oleifera leaves in Ugandan rural communities," Journal of Medicinal Plants Research, vol. 4, pp. 753-757, 2010.
4. N. Subasree, J. Arockiaselvi, P. Kamaraj and M. Arthanareeswari, "Study of mild steel corrosion in sulphuric acid medium by moringa oleifera leaf extract by electrochemical and surface analysis studies," International journal of chemtech research, vol. 11, pp. 317-325, 2018.
5. Ayende, F. Rachmanda, J. W. Soedarsono, D. Priadi and Sulistijono, "Corrosion Behavior of API-5L in Various Green Inhibitors," Advanced Materials Research, Vols. 634-638, pp. 689-695, 2013.
6. A. Y. El-Etre and A. I. Ali, "A novel green inhibitor for C-steel corrosion in 2.0 mol•L−1 hydrochloric acid solution," Chinese Journal of Chemical Engineering, vol. 25, pp. 373-380, 2017.
7. A. A. Olajire, "Corrosion inhibition of offshore oil and gas production facilities using organic compound inhibitors - A review," Journal of Molecular Liquids, vol. 248, pp. 776-808, 2017.
8. M. F. Azmi and J. W. Soedarsono, "Study of corrosion resistrance of pipeline API 5L X42 using green inhibitor bawang dayak (Eleutherine americanna Merr.) in 1M HCl," in 2nd international Tropical Renewable Energy Conference (i-TREC), 2017.
9. Ayende, A. Rustandi, J. W. Soedarsono, D. Priadi, Sulistijono, D. N. Suprapta, G. Priyotomo and R. Bakri, "Effects of Purple Sweet Potato Extract Addition in Ascorbic Acid Inhibitor to Corrosion Rate of API 5L steel in 3.5% NaCl Environment," Applied Mechanics and Materials, vol. 709, pp. 384-389, 2014.
10. M. A. Ibraheem, A. E. A. El Sayed Fouda, M. T. Rashad and F. N. Sabbahy, "Sweet Corrosion Inhibition on API 5L Pipeline Steel," International Scholarly Research Network Metallurgy, vol. 2012, 2012.
11. M. H. Hussin and M. J. Kassim, "The corrosion inhibition and adsorption behavior of Uncaria gambir extract on mild steel in 1M HCl," Materials Chemistry and Physics, vol. 125, pp. 461-468, 2011.
12. J. R. Macdonald and W. B. Johanson, Theory in Impedance Spectroscopy, New York: John Wiley & Sons, 1987.
13. F. Bentiss, M. Traisnel and M. Lagrence, "The substituted 1,3,4-oxadiazoles: a new class of corrosion inhibitors of mild steel in acidic media," Corrosion Science, vol. 42, pp. 127-146, 2000.
14. K. Zhang, W. Yang, B. xu, Y. Chen, X. Yin, Y. Liu and H. Zuo, "Inhibitory effect of konjac glucomanan on pitting corrosion of AA5052 aluminium alloy in NaCl solution," Journal of Colloid and Interface Science, vol. 517, pp. 52-60, 2018.
15. M. Ozcan, R. Solmaz, G. Kardas and I. Dehri, "Adsorption properties of barbiturates as green corrosion inhibitors on mild steel in phosphoric acid," Colloids and Surfaces A: Physicochemical and Engineering Aspects, vol. 325, pp. 57-63, 2008.

16. A. E. S. Fouda, F. I. El Dossoki, M. F. Atia, F. M. A. E. Aziz and A. El Hossiany, "Contribution to the corrosion inhibition of aluminum by aqueous extract of Moringa oleifera in 2 M HCl," Discover Chemical Engineering, 2025.
17. A. Wijaya, J. W. Soedarsono, A. P. Laksana and T. Aditiyawarman, "Study of mixing purple sweet potato and turmeric extract as green corrosion inhibitor for API-5L in NaCl 3,5% environment," AIP Conference Proceedings, 2023.
18. Y. Teng, W. Zhang, M. Wang, C. Yu, Y. Ma, J. Bian, X. Yang and D. Zhang, "Anthocyanin as sustainable and non-toxic corrosion inhibitor for mild steel in HCl media: Electrochemical, surface morphology and theoretical investigations," Journal of Molecular Liquids, 2021.
19. Z. Zhang and X. Feng, "Synthesis and evaluation of new type plant extraction corrosion inhibitor," Geoenergy Science and Engineering, 2025.
20. Supratman, "Efektifitas ekstrak biji keluak (Pangium Edule Reinw) dan ubi ungu (Ipomoea Batatas) sebagai green corrosion inhibitor pada material baja API 5L dalam larutan 0,2M HCl (Tesis Magister)," 2019.
21. S. Prifiharni, G. Mashanafie, G. Priyotomo, A. Royani, A. Ridhova, B. Elya and J. W. Soedarsono, "Extract sarampa wood (Xylocarpus Moluccensis) as an eco-friendly corrosion inhibitor for mild steel in HCl 1M," Journal of the Indian Chemical Society, 2022.
22. M. E. Eissa, S. H. Etaiw, E. S. El-Hussieny, A. A. El Hossiany and A. E.-A. S. Fouda, "Sweet Orange Peel Extract as green sustainable corrosion inhibitor for Al in 1 M HCl," International Journal of Electrochemical Science, 2025.
23. G. N. Chukwueze, C. O. Asadu, C. E. Onu and I. S. Ike, "Evaluation of the Corrosion Inhibitive Properties of Three Different Leave Extracts on Mild Steel Iron in Sulphuric Acid Solution," Journal of Engineering Research and Reports, 2020.
24. A. B. D. Nandiyanto, R. Ragadhita and M. Fiandini, "Interpretation of Fourier Transform Infrared Spectra (FTIR): A Practical Approach in the Polymer/Plastic Thermal Decomposition," Indonesian Journal of Science & Technology, 2023.
25. I. A. Bouabdallah, F. Adjal, A. Zaabar, A. Benchikh, D. Guerniche, C. A. Ramdane-Terbouche, A. P. Piedade, M. Z. Ibrahim, N. Nasrallah and A. Abdi, "Cleome arabica L. extract as a novel green corrosion inhibitor for AISI 1045 carbon steel in 0.5 M HCl: insights from experimental and theoretical DFT analyses," RSC Advances, 2024.
26. K. H. Rashid, A. A. Khadom and S. H. Abbas, "Optimization, kinetics, and electrochemical investigations for green corrosion inhibition of low-carbon steel in 1 M HCl by a blend of onion-garlic leaves wastes," Bioresource Technology Reports, 2022.
27. A. P. S. Kaban, W. Mayangsari, M. S. Anwar, A. Maksum, R. Riastuti, T. Aditiyawarman and J. W. Soedarsono, "Experimental and modelling waste rice husk ash as a novel green corrosion inhibitor under acidic environment," Materials Today: Proceedings, 2022.
28. J. W. Soedarsono, M. N. Shihab, M. Fikri and A. Maksum, "Study of curcuma xanthorrhiza extract as green inhibitor for API 5L X42 steel in 1M HCl solution," IOP Conference Series: Earth and Environmental Science, 2018.